Seismic attenuation in partially saturated rocks: Recent advances and future directions

Nicola Tisato, previously at ETH Zurich; currently at University of Toronto
Beatriz Quintal and Samuel Chapman, University of Lausanne
Claudio Madonna, Shankar Subramaniyan, Marcel Frehner, and Erik H. Saenger, ETH Zurich
Giovanni Grasselli, University of Toronto

Abstract

The large amount of data collected with the broadband attenuation vessel (BBAV) and other laboratory devices and analyzed in the last five years sheds light on the physics of wave-induced fluid flow in Berea Sandstone. However, the knowledge is insufficient to fully exploit the physics of seismic wave attenuation in partially saturated rocks. In particular, some technical challenges have limited the depth of research. Soon these challenges will be overcome by the use of fluid-pressure sensors capable of measuring wave-induced fluid pressure in the seismic bandwidth when the sample is under high confining pressures. In addition, a new subresonance apparatus, paired with a micro-CT system, will be used to further investigate the influence of fluid distribution and microstructural features on attenuation.

Introduction

In the last decade, an increasing number of studies has focused on the determination of anelastic properties of geomaterials (e.g., Adam et al., 2009; Mikhaltsevitch et al., 2011; Tisato and Madonna, 2012; Madonna and Tisato, 2013). Complex elastic moduli and therefore attenuation are of great interest to the industry also because new energy resources are stored in highly attenuating materials such as gas shales and bitumen sands. Indeed, seismic tomography has been improved lately by using the analysis of attenuation to characterize subsurface domains (e.g., Goodway et al., 2012).

During the last five years, the rock-physics research group at ETH Zurich (ROCKETH) has developed two apparatuses to measure seismic attenuation in the extensional mode (Tisato and Madonna, 2012; Madonna and Tisato, 2013). These apparatuses have been used intensively to study attenuation related to the Young's modulus ($1/Q_E$) in partially saturated Berea Sandstone and to verify a wave-induced fluid-flow model, which explains the observed attenuation.

In fact, because of the special design and the combination of laboratory results with 3D numerical modeling based on poroelasticity, we demonstrated that wave-induced fluid flow on the mesoscopic scale can cause significant frequency-dependent attenuation in partially saturated Berea Sandstone samples (e.g., Tisato and Quintal, 2013a). However, such studies are limited by approximations concerning fluid distribution but could be extended if technological improvements are undertaken.

The present contribution reports on (1) the development of the broadband attenuation vessel (BBAV) (Tisato and Madonna, 2012), (2) the most significant results obtained so far, (3) upgrades of the laboratory device, and (4) a new pilot project that sheds more light on the still rather obscure physics of attenuation.

The broadband attenuation vessel

The broadband attenuation vessel (BBAV) was developed at ETH Zurich starting in the second half of 2009 and was completed in 2010. The vessel can host a large cylindrical rock sample (76-mm diameter, 250-mm length), on which it can exert a confining pressure of as much as 25 MPa via high-pressure oil. The sample is isolated from the confining medium by aluminum foil glued onto the sample and a fluorinated ethylene propylene (FEP) shrink tube. This avoids attenuation caused by open-pore boundary condition, which would be negligible anyway for the used sample, fluid types, and conditions (Tisato and Madonna, 2012).

The BBAV is hosted in a uniaxial press driven by a servoelectric uniaxial actuator that applies vertical stress on the sample (σ_V) (Figure 1). A piezoelectric motor controlled by a high-voltage amplifier generates a sinusoidal variation of σ_V necessary to estimate the complex Young's modulus (E_Z). This modulus

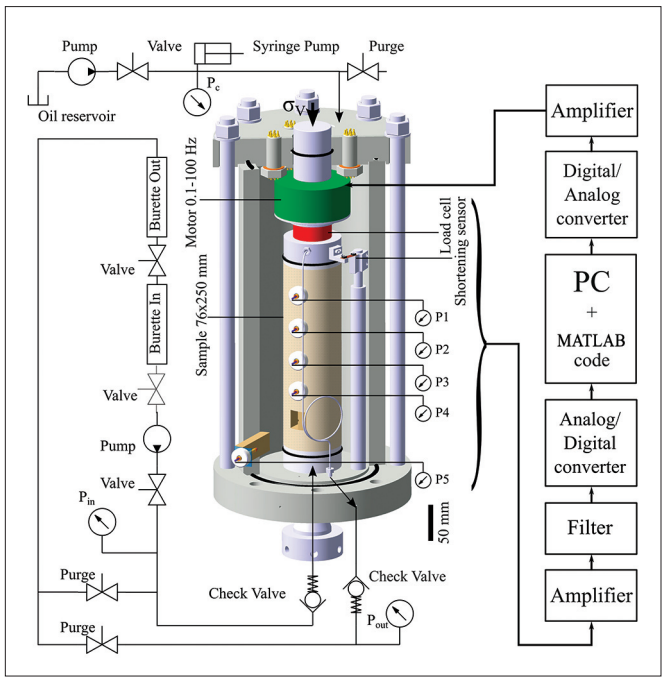

Figure 1. Schematic illustration of the broadband attenuation vessel (BBAV). The apparatus can confine a cylindrical sample (76 × 250 mm) as high as 25 MPa. The BBAV is used to measure the real part of the Young's modulus and its related attenuation (E and $1/Q_E$) in addition to transient fluid pressures at five sensor locations, P1 through P5 (Tisato and Madonna, 2012; Tisato and Quintal, 2013a).

is calculated according to the sinusoidal force and shortening. In fact, a load cell placed between the motor and the sample measures the sinusoidal force, and a cantilever measures the sinusoidal bulk vertical shortening of the sample. Knowing the areas of the end-faces and the length of the sample, it is possible to calculate the sinusoidal stress (σ) and strain (ε). Attenuation related to the Young's modulus can be calculated as

$$1/Q_E = \tan(\varphi), \quad (1)$$

where φ is the phase shift between σ and ε. Furthermore, the real part of the Young's modulus, here referred to simply as E, is obtained as (Lakes, 2009)

$$E = \frac{\sigma}{\varepsilon}\cos(\varphi). \quad (2)$$

Such subresonance apparatuses have to be calibrated by measuring materials with established attenuation. The BBAV was calibrated by testing aluminum alloy (AW-6082) and PMMA (i.e., Plexiglas) (Figure 2). The calibration indicates that the BBAV can accurately measure $1/Q_E$ between 0.003 and 0.1 (Tisato and Madonna, 2012). Moreover, the attenuation and dispersion curves obtained with the BBAV obey the Kramers-Kronig relation, indicating that the apparatus also yields accurate measurements of the dispersion of the real part of Young's modulus.

The large dimensions of the samples used in the BBAV allow the drilling of five holes along the length of the specimen with 42-mm spacing and 38-mm depth (Figure 1) (Tisato and Quintal, 2013a). The holes host five pore-fluid pressure sensors which are differential, zero volume, and 200-kPa full scale. Moreover, such sensors are 2 mm in diameter and react to pressure variations in less than 50 μs. Using this setup, we investigate the transient fluid pressures (and fluid-pressure gradients along the sample) caused by a variation of vertical stress and the resulting wave-induced fluid flow.

$1/Q_E$ of partially saturated Berea Sandstone

Berea Sandstone was tested under a wide range of conditions. In fact, since 2009, we have collected more than 100 seismic-attenuation and velocity-dispersion curves for Berea Sandstone with the BBAV. The effect of confining pressure on $1/Q_E$ was tested between 0.1 and 24 MPa, and pore-fluid saturation was varied between 0% and 97%, using water and a glycerin-water mixture with a viscosity of 11 mPa·s (GW-mix). However, results concerning GWmix-saturated cases are a matter of ongoing research and thus are not reported here.

Both dry Berea Sandstone and aluminum alloy exhibit frequency-independent attenuation. However, whereas for aluminum alloy, Q_E is always larger than 300, dry Berea Sandstone is more strongly attenuating with $Q_E \sim 100$ and ~ 200 for low and high confining pressures, respectively (Tisato et al., 2013). These results are in agreement with literature data (e.g., Winkler et al., 1979).

Further, we identified a significant frequency-dependent attenuation ($1/Q_E$ as low as 0.1) when Berea Sandstone was saturated with two fluid phases (i.e., water-air saturation). In fact, attenuation was frequency dependent only for saturations > 60% and confining pressure ≤ 10 MPa (Figure 2). We also measured ultrasonic wave speeds on the same samples (not shown here), which allowed us to investigate the "unrelaxed" state. Those measurements suggested that wave-induced fluid flow might be responsible for high and frequency-dependent attenuation (Tisato et al., 2013).

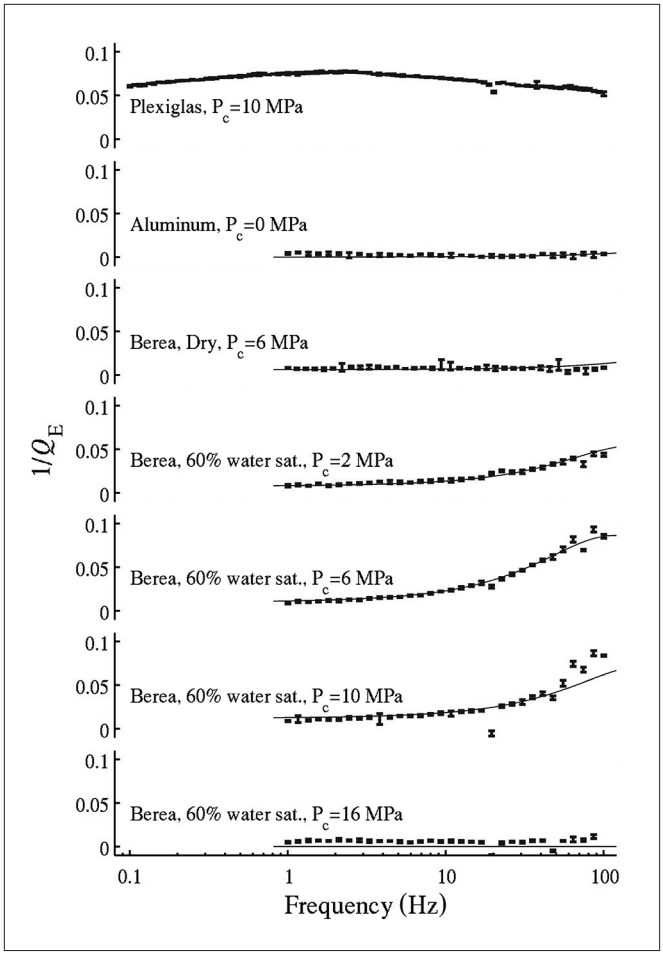

Figure 2. Attenuation ($1/Q_E$) measured in the bandwidth of 0.1 Hz to 100 Hz for different materials. Plexiglas and aluminum were used to calibrate the BBAV. Dry Berea Sandstone exhibits a frequency-independent $1/Q_E$, whereas partially saturated Berea Sandstone has a frequency-dependent attenuation for confining pressure (P_c) ≤ 10 MPa. Frequency-dependent attenuation varying with P_c might indicate a variation of solid-fluid interaction (Tisato and Madonna, 2012; Tisato et al, 2013). Data are fitted with the Kramers-Kronig relation, which links $1/Q_E$ to the modulus (i.e., E) dispersion (not shown here).

Transient fluid-pressure measurements

The study of wave-induced fluid flow was extended by measuring the fast variation of fluid pressure caused by a sudden increase of σ_V and the subsequent fluid-pressure equilibration along the sample. The applied step stress caused a strain (ε) of $\sim 10^{-6}$, which is similar to that generated by a propagating seismic wave. In dry Berea Sandstone, no pressure increase was measured after the step stress was applied, which is expected, given the high compressibility of the saturating gas (i.e., air). This result also indicates that the

rock-frame deformation does not confound the measured pressure signals.

Then the sample was saturated by injecting water from the bottom. For such a condition, the increase of fluid pressure, caused by the step stress, was significant (Figure 3). We estimated a saturation profile along the sample based on (1) the value of pressure recorded immediately after the step of stress and (2) the known total water saturation of 97%. This saturation profile was used to create several 3D models of patchy saturated samples (i.e., distribution of air- and water-saturated domains).

Quasi-static numerical creep tests solving Biot's equations of consolidation were performed on these 3D models (Quintal et al., 2011), yielding synthetic transient fluid-pressure and attenuation curves, which were then compared with laboratory data. Distribution and dimensions of the saturation patches (air-saturated domains) were varied manually up to the point when the mismatch between the calculated and the measured fluid-pressure transient was minimized. The computed attenuation was related only to wave-induced fluid flow on the mesoscopic scale ($1/Q_{fluid}$).

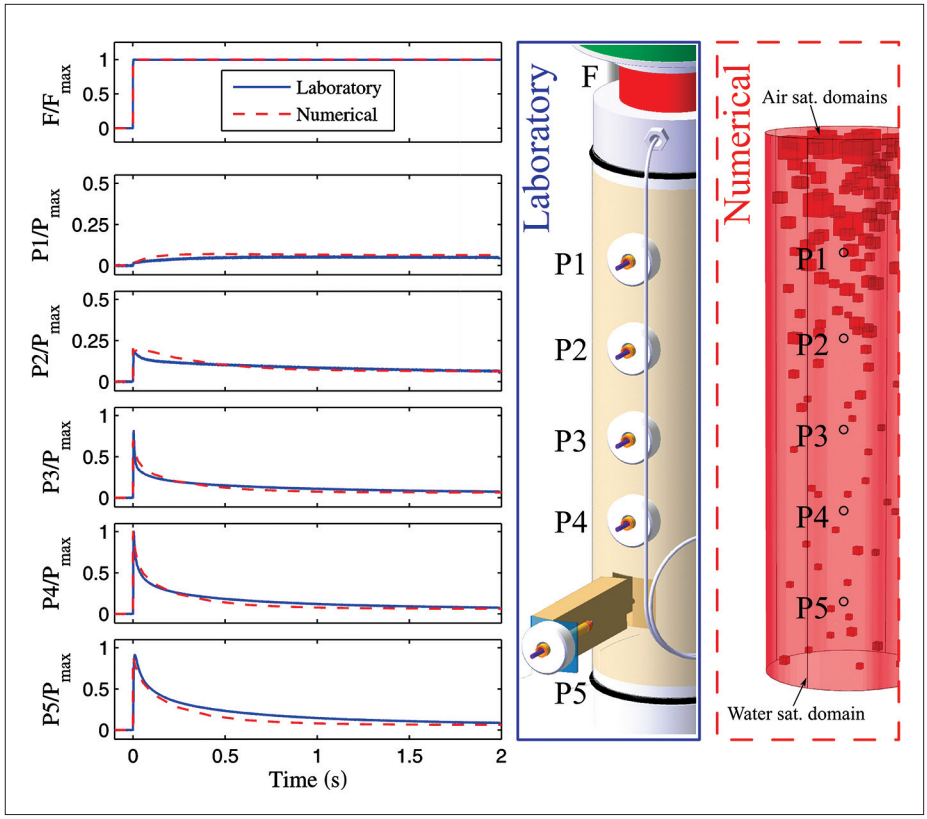

Figure 3. Transient fluid pressures P1 through P5 (also in Figure 1) measured by the BBAV and numerically calculated at five positions along a Berea Sandstone sample when a step force (F) is applied on top of the cylindrical sample. The sample was confined at 0.2 MPa, 97% saturated with water, and fluid distribution in the numerical model was based on laboratory measurements of fluid pressure (blue curves) at times close to 0 s. Numerical simulations described laboratory results well (Tisato and Quintal, 2013a).

We assumed that attenuation resulting from matrix anelasticity was equal to the value measured at dry conditions ($1/Q_{dry}$) and occurred also in measurements related to the fluid-saturated sample (Johnston et al., 1979). In addition, we considered $1/Q_{fluid}$ independent of $1/Q_{dry}$, and we calculated the total attenuation as

$$\frac{1}{Q_{total}} = \frac{1}{Q_{fluid}} + \frac{1}{Q_{dry}}. \qquad (3)$$

The value of $1/Q_{total}$ based on the results of the numerical simulation accurately fits the attenuation measured in the BBAV (Figure 4).

Because the transient fluid pressure also was fitted for the same model, it was possible to relate the mesoscopic-scale fluid flow to the amount of attenuation. This indicates that most of the frequency-dependent attenuation, measured in the 97% water-saturated sample, was caused by wave-induced fluid flow on the mesoscopic scale (Tisato and Quintal, 2013a).

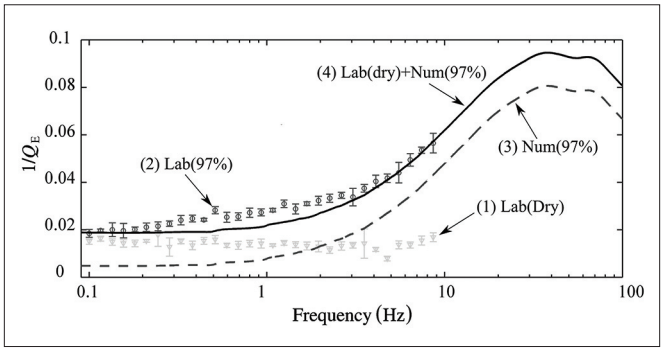

Figure 4. The numerical model, for which the measured transient pressure was fitted (Figure 3), yields also a $1/Q_E$ curve that fitted the measured data, confirming that wave-induced fluid flow on the mesoscopic scale is responsible for most of the frequency-dependent attenuation in the seismic bandwidth (Tisato and Quintal, 2013a). Curve (4) is given by the sum of the frame-related attenuation (1), measured at dry conditions ($1/Q_{dry}$), and the numerically calculated attenuation caused by wave-induced fluid flow on the mesoscopic scale (3).

Strain dependence

We also investigated the influence of the vertical strain magnitude on the attenuation and on the transient fluid pressures. Tests were performed for dry and water-saturated samples and for strains between $\varepsilon_1 = 0.8 \times 10^{-6}$ and $\varepsilon_2 = 1.9 \times 10^{-5}$. Here, considering constant strain, we assume that the frame-related attenuation (i.e., $1/Q_{dry}$) is independent on the saturation conditions. The subtraction of attenuation curves obtained at different strains but the same saturation (including the dry condition) yields

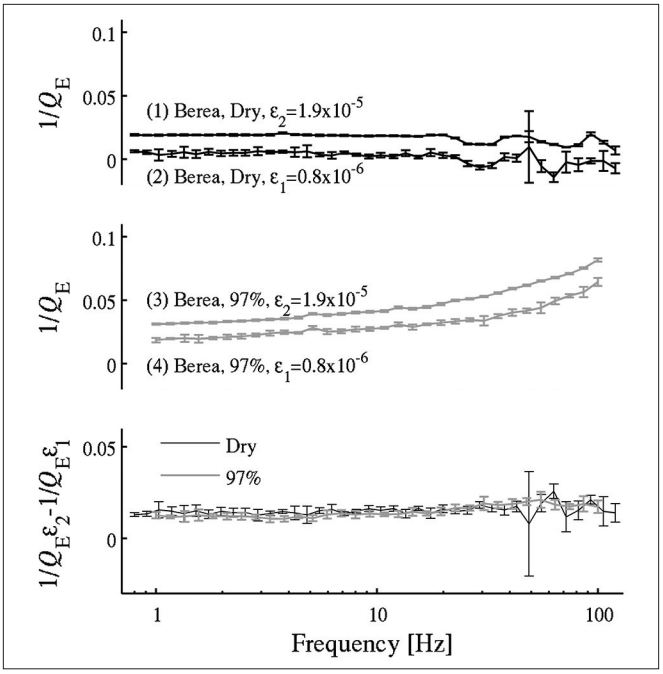

Figure 5. The BBAV was used to investigate the influence of strain on attenuation. For increasing strain, measurements on Berea Sandstone at dry and partially saturated conditions show a similar increase in attenuation, indicating that for the considered strains, fluid-related attenuation is approximately independent of strain (Tisato and Quintal, 2013b).

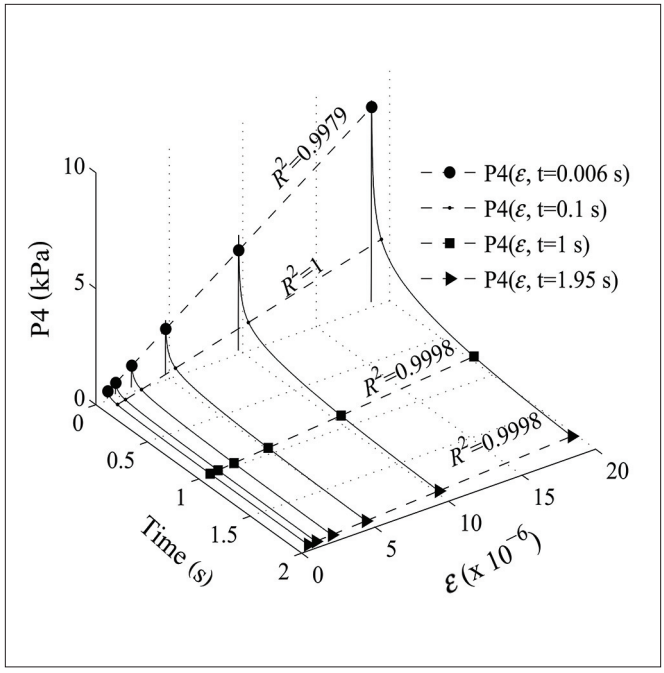

Figure 6. Transient fluid pressures measured at strains ranging between 0.8 × 10^{-6} and 1.9 × 10^{-5} in Berea Sandstone saturated with 97% water. For a specific time, fluid pressure increases linearly with strain. This observation confirms that fluid-related attenuation is independent of strain.

similar and frequency-independent curves (Figure 5). Moreover, the increase of attenuation, caused by the increase of strain, agrees with the literature (Winkler et al., 1979). This indicate that regardless of the saturation, the higher the strain magnitude, the larger the attenuation, whereas the frequency-dependent part of the signal, which represents the fluid-related attenuation (i.e., wave-induced fluid flow), is conserved. This suggests that the fluid-related ($1/Q_{fluid}$) and solid frame-related attenuation (i.e., $1/Q_{dry}$) are independent from each other and that $1/Q_{fluid}$ is not influenced significantly by strain magnitude. In other words, we conclude that the attenuation increase is caused only by the frame-related attenuation increase. This is supported by the fact that the fluid-pressure measurements depend linearly on strain (Figure 6) (Tisato and Quintal, 2013b). All these experiments corroborate the assumptions made in equation 3 above (Johnston et al., 1979).

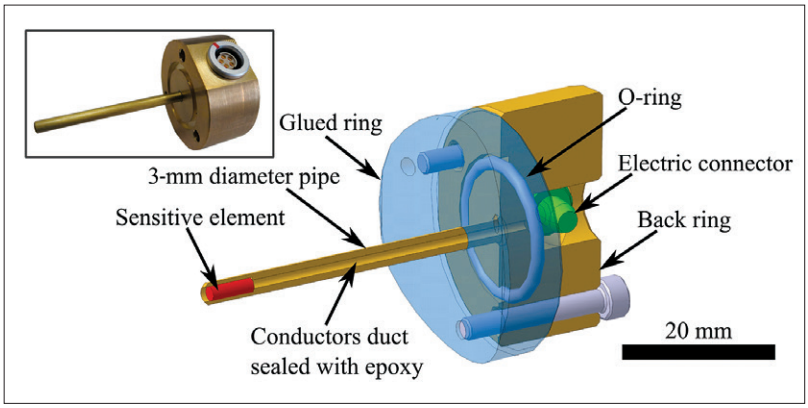

Figure 7. Fluid-pressure sensor, capable of withstanding high confining pressure, designed and built (see inset) to investigate why frequency-dependent attenuation is reduced or vanishes at high confining pressures (Figure 2).

Discussion

Combining laboratory measurements and numerical modeling, we have demonstrated for the first time that wave-induced fluid flow on the mesoscopic scale is responsible for large and frequency-dependent seismic attenuation measured in a decametric-sized Berea Sandstone sample partially saturated with water (Tisato and Quintal, 2013a). We also have reported significant relations between attenuation and confining pressure and between attenuation and strain (Tisato et al., 2013; Tisato and Quintal, 2013b).

Because of the use of differential fluid-pressure sensors, with the current setup, it is impossible to measure transient fluid pressures for high confining pressure (i.e., > 0.2 MPa). Measuring fluid pressure at high confining pressures is important to explain why frequency-dependent attenuation vanishes for confining pressures > 10 MPa (Figure 2). Wave-induced fluid-flow theories predict decreasing attenuation for increasing confining pressures (i.e., increasing frame stiffness).

Moreover, it is well known that deformation of the internal structure of rocks, induced by a variation of vertical stress, is a function of confinement (e.g., formation of conjugate shear bands at high confining pressures). Therefore, the interaction between frame and fluid and the resulting attenuation

might vary as the confining pressure changes (Tisato et al., 2013). Nevertheless, to scientifically prove our hypotheses, we tried to overcome such a limitation by designing, building, and testing new absolute fluid-pressure sensors capable of withstanding high confining pressures (Figure 7).

These sensors will be used to measure transient fluid pressures in partially saturated rocks and high confining pressures (i.e., > 0.2 MPa). For each variation in the frequency-dependent attenuation, we also expect to find a variation in the fluid-pressure response. Such tests also will allow us to numerically verify our hypothesis and to enrich further the knowledge about wave-induced fluid flow.

The inability to image the fluid distribution within the Berea Sandstone forced Tisato and Quintal (2013a, 2013b) to estimate it indirectly. However, the ongoing project Experimental Rock Deformation Under μCT – (ERDμ), funded by the Swiss National Science Foundation, will combine the micro-CT system at the University of Toronto (Phoenix|X-rayv|tome|x) and a newly designed X-ray transparent subresonance apparatus (Figure 8) to measure the complex Young's modulus while imaging the internal structure of the sample. Such a device will reveal details of fluid distribution and will allow better understanding of the physics of attenuation.

We also will study the complex Young's modulus as a function of the internal rock-frame microstructure. To this end, the main plan is to inject CO_2 to enhance dissolution or precipitation of mineral phases and to force microstructural modifications. Attenuation will be measured to study the influence on elasticity of such modifications.

Our research will aid seismic tomography of subsurface domains to provide information about fluid and rock properties of geomaterials, based on their relationship with attenuation, especially for cases in which the reservoir is subjected to CO_2 injection, exploitation of geothermal energy, and extraction of hydrocarbons.

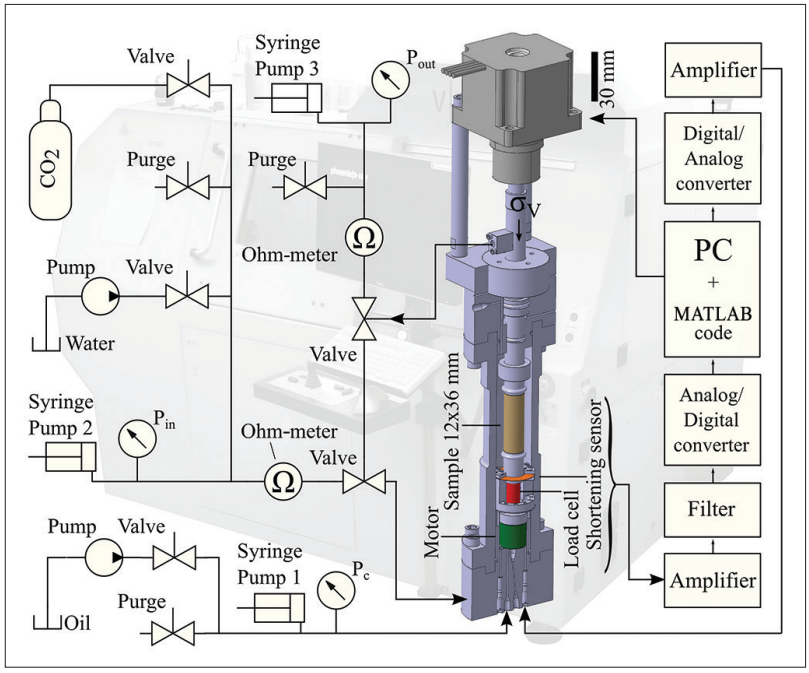

Figure 8. Schematic of the newly designed vessel called ERDμ, which is X-ray transparent. A micro-CT (in the background) can be used to image the confined sample simultaneously to the measurement of seismic attenuation. The ERDμ can confine a sample 12 × 36 mm as high as 30 MPa.

Conclusion

The large amount of data collected with the BBAV and other laboratory devices and analyzed in the last five years allowed us to shed light on the physics of wave-induced fluid flow in Berea Sandstone. Nevertheless, the gained knowledge is insufficient to fully exploit the physics of seismic wave attenuation in partially saturated rocks. In particular, some technical challenges have limited the depth of our research; for example, we lack detailed information about fluid distribution or measurement of fluid pressure at high confining pressures.

Soon these challenges will be overcome by the use of already built new fluid-pressure sensors capable of measuring wave-induced fluid pressure in the seismic bandwidth when the sample is under high confining pressures. In addition, a new subresonance apparatus, paired with a micro-CT system, will be used to further investigate the influence of fluid

distribution and microstructural features on attenuation. These developments will help to further uncover the physics of seismic wave attenuation in porous materials. TLE

References

Adam, L., M. Batzle, K. T. Lewallen, and K. van Wijk, 2009, Seismic wave attenuation in carbonates: Journal of Geophysical Research, **114**, no. B6, B06208, http://dx.doi.org/10.1029/2008JB005890.

Goodway, B., D. Monk, M. Perez, G. Purdue, P. Anderson, A. Iverson, V. Vera, and D. Cho, 2012, Combined microseismic and 4D to calibrate and confirm surface 3D azimuthal AVO/LMR predictions of completions performance and well production in the Horn River gas shales of NEBC: The Leading Edge, **31,** no. 12, 1502–1511, http://dx.doi.org/10.1190/tle31121502.1.

Johnston, D. H., M. N. Toksöz, and A. Timur, 1979, Attenuation of seismic waves in dry and saturated rocks: II. Mechanisms: Geophysics, **44,** no. 4, 691–711, http://dx.doi.org/10.1190/1.1440970.

Lakes, R., 2009, Viscoelastic materials: Cambridge University Press.

Madonna, C., and N. Tisato, 2013, A new seismic wave attenuation module to experimentally measure low-frequency attenuation in extensional mode: Geophysical Prospecting, **61,** no. 2, 302–314, http://dx.doi.org/10.1111/1365-2478.12015.

Mikhaltsevitch, V., M. Lebedev, and B. Gurevich, 2011, A low-frequency laboratory apparatus for measuring elastic and anelastic properties of rocks: 81st Annual International Meeting, SEG, Expanded Abstracts, 2256–2260, http://dx.doi.org/10.1190/1.3627657.

Quintal, B., H. Steeb, M. Frehner, and S. M. Schmalholz, 2011, Quasi-static finite element modeling of seismic attenuation and dispersion due to wave-induced fluid flow in poroelastic media: Journal of Geophysical Research, **116,** no. B1, B01201, http://dx.doi.org/10.1029/2010JB007475.

Tisato, N., and C. Madonna, 2012, Attenuation at low seismic frequencies in partially saturated rocks: Measurements and description of a new apparatus: Journal of Applied Geophysics, **86,** 44–53, http://dx.doi.org/10.1016/j.jappgeo.2012.07.008.

Tisato, N., and B. Quintal, 2013a, Measurements of seismic attenuation and transient fluid pressure in partially saturated Berea Sandstone: Evidence of fluid flow on the mesoscopic scale: Geophysical Journal International, **195,** no. 1, 342–351, http://dx.doi.org/10.1093/gji/ggt259.

Tisato, N., and B. Quintal, 2013b, Transient fluid pressure and attenuation measurements: Strain versus saturation: Second International Workshop on Rock Physics.

Tisato, N., C. Madonna, and E. H. Saenger, 2013, Seismic wave attenuation for partially saturated sandstone as a function of confining pressure: 83rd Annual International Meeting, SEG, Expanded Abstracts, 2626–2631, http://dx.doi.org/10.1190/segam2013-0301.1.

Winkler, K., A. Nur, and M. Gladwin, 1979, Friction and seismic attenuation in rocks: Nature, **277,** no. 5697, 528–531, http://dx.doi.org/10.1038/277528a0.

Acknowledgments: Our work has been supported by the Swiss Commission for Technology and Innovation (CTI), the Low Frequency Seismic Partnership (LFSP), and the Swiss National Science Foundation (SNSF). We thank Robert Hofmann, Reto Seifert, and Jeff Sansome for providing many technical solutions for our laboratory problems, all the other members of ROCKETH for positive scientific interaction, and Ludmila Adam and Kasper Van Wijk for helping to improve the quality of this article.

Corresponding author: nicola.tisato@utoronto.ca